Received: 23 March 2021 | Revised: 8 September 2021 | Accepted: 11 September 2021

DOI: 10.1002/esp.5250

RESEARCH ARTICLE

ESPL WILEY

Basin-wide hydromorphological analysis of ephemeral streams using machine learning algorithms‡

Maria Pilar Rabanaque[1] | Vanesa Martínez-Fernández[1] | Mikel Calle[2] | Gerardo Benito[1]

[1]Department of Geology, National Museum of Natural Sciences (MNCN), CSIC, Madrid, Spain

[2]Department of Geography and Geology, University of Turku, Turku, Finland

Correspondence
Maria Pilar Rabanaque, Department of Geology, National Museum of Natural Sciences (MNCN), CSIC, Serrano 115 bis, 28006, Madrid, Spain.
Email: m.rabanaque@mncn.csic.es

Funding information
Post-doc Juan de la Cierva programme, Grant/Award Number: FJC2018-035451-I; PhD FPI programme, Grant/Award Number: PRE2018-086771; EPHIDREAMS, Grant/Award Number: PID2020-116537RB-I00; EPHIMED, Grant/Award Number: CGL2017-86839-C3-1-R

Abstract

Sustainable river management now encompasses a much wider concept that includes hydromorphological and fluvial habitat studies. In ephemeral streams, the geomorphological characterization of channels is complex due to episodic flows and riparian vegetation dynamics. Stream channel survey and classification at the watershed scale provide the basis for geomorphological conservation, process interpretation, assessing sensitivity to disturbance, and identifying reaches that supply and store sediment. Here, we present a stream classification based on a two-step approach: (1) automatic river segmentation based on spatial variability in channel/valley morphology from topographic measurements (LiDAR, light, detection and ranging), and (2) fluvial landform and vegetation density mapping derived from multispectral open-source satellite images (Sentinel-2) using support vector machine (SVM) and Random Forest (RF) algorithms. These analyses provide continuous, quantitative spatial values of geometric (channel/valley width, slope gradient, and route distance), landform (active channel and gravel bars with five densities of vegetation cover), and hydraulic (specific stream power) variables. Four stream types were identified in the Rambla de la Viuda catchment (~1500 km^2), an ephemeral gravel-bed river in eastern Spain. The spatial distribution of channel types is explained by differences in geometry (active channel width, valley width, and slope gradient) and a hydraulic parameter (specific stream power). The landforms/vegetation patterns provided insight on causal relationships between erosion and deposition processes during high flow periods and the time since the most recent large disruptive flood event. Channel type distribution provided first-order predictions about the location of reaches that supply and store sediment and thus information on sediment continuity along the river. Dam effects on downstream reaches resulted in geomorphological disequilibrium, producing narrowing of the active channel, slope reduction, and a decrease of gravel bar areal extension. The proposed catchment scale analysis provides a comprehensive and replicable methodology for environmental planning in Mediterranean ephemeral streams to guide further hydromorphological surveys at the reach scale.

KEYWORDS
ephemeral rivers, geomorphological assessment, machine learning, network segmentation, remote sensing, river management, stream classification

‡Tribute to Professor Ken Gregory.

1 | INTRODUCTION

Intermittent rivers and ephemeral streams (IRES; Datry et al., 2017) account for over 50% of the total length of the global river network (Skoulikidis et al., 2017) and comprise a large portion of Mediterranean watersheds. The extension of Mediterranean IRES is expected to increase in the near future, as some perennial rivers are experiencing intermittency due to climate change, land-use changes, and water demands (Gallart et al., 2012). Over the last few years, increasing efforts have been made to update methods for the operational monitoring, assessment, and classification of the water regime, biodiversity, and ecological functions of IRES (Datry et al., 2014; Datry et al., 2018; Leigh et al., 2016). These studies recognize the importance of the biophysical structure (e.g., channel morphology, substrate composition) and the eco-hydrological processes that support ecosystem functions (Datry et al., 2018). In dryland regions, physical and biological processes are more diverse and complex than their perennial counterparts due to inherent differences in climate, hydrology, geology, physiography, and human activities (Jaeger et al., 2017). Therefore, the assessment of their hydrological regime, network connectivity and geomorphological conditions is a challenging task (Gallart et al., 2017; Skoulikidis et al., 2017).

Recently, river management has adopted a hydromorphological approach [e.g., European Union (EU) Water Framework Directive, European Commission, 2000, 2003) to evaluate integrated aspects of geomorphology, hydrology, and freshwater ecology in preserving the important ecosystem services that rivers provide. Following a top-down watershed analysis, several frameworks for generating process-based understanding have been proposed for perennial rivers, namely the River Styles Framework (Brierley & Fryirs, 2005), IDRAIM (Rinaldi et al., 2015), or the multi-scale hierarchical framework (Gurnell et al., 2016) with all of them requiring a river segmentation frequently based on expert criteria before river characterization. However, specific approaches for developing process-based understanding of hydromorphological conditions of ephemeral streams are still scarce (e.g., IHG-E in CHJ, 2018) or mostly related with the evaluation of the biological component of the fluvial system (i.e., TREHS in Gallart et al., 2017). The hydromorphological approaches to stream segmentation are critical in assessing the environmental conditions of Mediterranean ephemeral streams and is the necessary stage for the consequent understanding of geomorphological dynamics across different spatial and temporal scales.

Ideally, a hydromorphological assessment should include a catchment morphological survey to evaluate the spatial and temporal links between flow regime and landform as part of the river's environmental characteristics (England & Gurnell, 2016). In most cases, existing geomorphological surveys are limited and catchment-scale data collection becomes costly (Downs & Thorne, 1996). As such, a Catchment Baseline Survey (CBS) is typically derived from the technique of geomorphological mapping with the support of topographic maps and aerial photographs (Cooke & Doornkamp, 1990; Hooke, 1997; Grabowski & Gurnell, 2016; Sear & Newson, 2010). Basin-wide analyses preferably include a combination of measurements of channel geometry, riparian land uses, channel dynamics, and evidence of previous management activity (Downs & Brookes, 1994). In perennial rivers, these surveys may be representative of channel conditions in the order of 10 to 100 years (Downs & Thorne, 1996), whereas in ephemeral streams with landforms controlled by episodic flooding the inferred interpretations may be limited to much shorter periods (Sanchis-Ibor et al., 2019). New approaches are therefore required to provide continuous, efficient, and replicable geomorphological data surveys at the catchment scale (Demarchi et al., 2020; Notebaert & Piégay, 2013; Piégay et al., 2020). Currently available open-access geospatial data, global positioning systems, and multispectral airborne and satellite images (e.g., Landsat, Sentinel) provide suitable datasets for repeated analysis at the catchment scale. For instance, a Pan-European riverscape unit mapping was recently produced based on Copernicus VHR Image Mosaic (2.5 m pixel) and the EU Digital Elevation Model (DEM) (25 m grid), although it is only applicable to large rivers (Demarchi et al., 2020). What is missing from this general riverscape analysis, however, is a hierarchical context for stream reach classification based on quantitative geometric and geomorphological variables at the catchment level. A need therefore exists for a methodological approach for the objective spatial analysis of Mediterranean ephemeral networks that could be used as a decision support tool to assess geomorphological functionality, response to disturbance, and connectivity along the river network.

The main objective of this article is to develop a basin-wide approach for ephemeral streams in support of sustainable river management, based on stream channel classification and open-source geospatial data. The specific objectives include: (1) to use objective criteria with a replicable methodology; (2) to provide objective delineation of functional river segments along the longitudinal continuum; (3) to generate an inventory of morphological and vegetation conditions at a reach scale that will subsequently be used to train machine learning algorithms; (4) to classify river channels based on their geometric, morphological and hydraulic characteristics; and (5) to identify river segments with degraded geomorphological conditions due to natural or human disturbance.

2 | STUDY AREA

Our study area is the Rambla de la Viuda, a Mediterranean ephemeral river that drains a catchment of ~1500 km^2 in eastern Spain (Figure 1). Rambla de la Viuda forms from two main tributaries, namely the Montlleó River and Rambla Carbonera, while the lower course is fed by the Llucena-Alcora River (Figure 1). The major tributaries of the Montlleó River are the Majó and Seco Rivers at the headwaters, and the Rambla Atzeneta and Benafigos streams in the lower part. Other tributaries include the Barranc dels Olles, Barranc Solana, and Rambla Estrets. The geology comprises three major zones: (1) the northern and north-western limit of the watershed is a northeast–southwest (NE–SW) mountainous relief (Iberian Range) with Cretaceous and Jurassic limestones and marls folded by the Alpine compressional cycle (Anadón & Moissenet, 1996); (2) a central belt of Neogene and Plio-Quaternary horst and grabens, partially infilled with Quaternary alluvium, running parallel to the coast corresponding to the present alluvial valley bottoms (Simón et al., 2013); and (3) the coastal plain formed by several levels of coalescent Quaternary alluvial fans that eroded previous horst reliefs next to the coast (Segura & Pardo-Pascual, 2019).

The climate is meso-Mediterranean in the upper catchment, which reaches 1250–1720 m above sea level (a.s.l.) (pine and

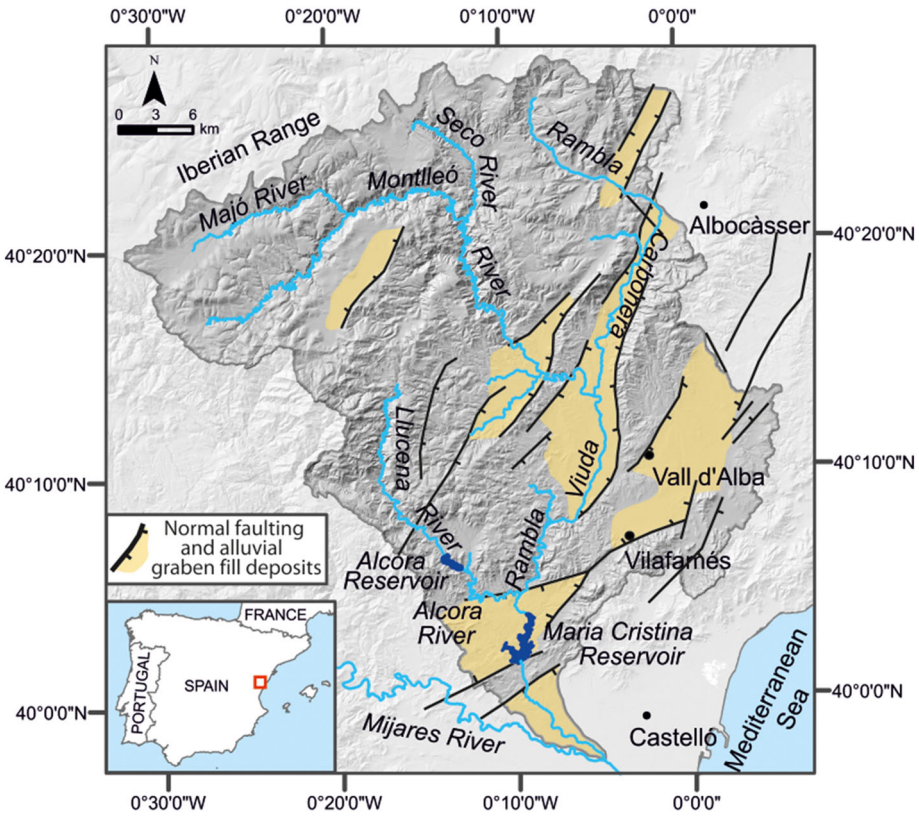

FIGURE 1 Location and topography of the study area

evergreen oak forests), and thermo-Mediterranean (shrublands) in the rest of the catchment, with a mean annual temperature of 9 to 15°C, daily winter minima below 0°C and summer maxima above 30°C. Precipitation varies from north to south across the basin, from annual values of ~750 mm/a in the Iberian Range to ~400 mm/a in the lower catchment near the Mediterranean Sea (Mateu, 1974). The main rainfall season occurs in autumn (September–November), with a second maximum in late winter to spring (March–May).

The discharge pattern is strongly marked by the seasonal rainfall regime, the high bedrock permeability due to the dominance of karstified limestones, and the high transmission losses affected by hyporheic flow interactions within wide Quaternary alluvial fill basins (Beneyto et al., 2020). Thus streamflow occurs during 31 d/yr on average, typically lasting 2–3 days, and stream runoff requires an accumulated rainfall episode larger than 70 mm (Camarasa & Segura, 2001). Intense rainfalls (i.e., up to 300 mm in 24 h) occur mainly in the autumn and are associated with mesoscale convective cells (Llasat & Puigcerver, 1990), eventually producing large floods with peak discharges in excess of 1500 m^3/s at Maria Cristina Reservoir (Benito et al., 2020; Machado et al., 2017). These floods contribute to this irregular hydrological regime, producing up to 80% of the annual discharge volume (Segura & Camarasa, 1996).

3 | METHODOLOGY

The methodology involves seven main phases (Figure 2): (1) preprocessing of satellite data from Sentinel-2 (i.e., calculation of spectral and textural indices); (2) manual collection of landform sample data for variable selection and supervised classification); (3) selection of spectral bands or indices for performing supervised classification; (4) data production from extraction of geomorphic variables using a geographic information system (GIS); (5) application of statistical methods to a set of selected independent variables to detect internally homogeneous segments significantly different from the adjacent segments; (6) cluster analysis of river segments based on geomorphic variables to identify river channel types; and (7) interpretation of fluvial geomorphology and stream functionality of the segment types (T) derived from the objective classification method.

3.1 | Data sources

3.1.1 | Remote sensing variables extraction from Sentinel-2

In order to develop our land cover analysis, a total of 16 remote sensing variables based on previous literature about land cover and land-use analysis (Borak, 1999; Marceau et al., 1990) were selected: six single spectral bands of Sentinel-2; three spectral indices; and seven textural indices. All of these data were cloud processed and downloaded from the Google Earth Engine (GEE) platform.

We performed the analysis using Sentinel-2 imagery with the advantage of its finer spatial resolution (10 m) in comparison to other open data satellite multispectral sensors (e.g., Landsat – 30 m). For this study, we selected Red, Green, Blue (RGB), NIR1, SWIR1, and SWIR2 as candidate variables with the two latter being resampled to 10 m using the bilinear interpolation method. We used a Level 2A surface reflectance product, filtering by date (15 June 2019) and tile (T30TYK). We selected this image because it had less than 10% cloud cover.

Spectral indices enhance the visibility of vegetation patches and are a powerful photosynthetic activity indicator. Specifically, we used the Normalized Difference Vegetation Index (NDVI) (Rouse

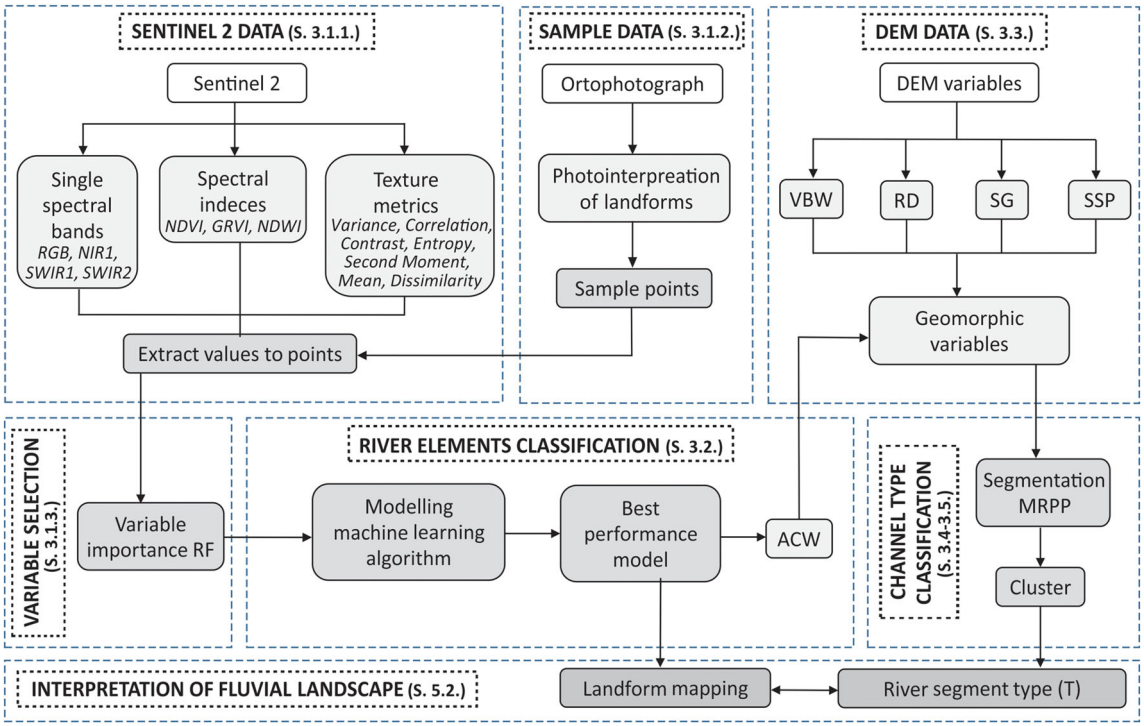

FIGURE 2 General workflow diagram used for landform mapping and typological river classification. VBW: valley bottom width; RD: route distance; SG: slope gradient; SSP: specific stream power; ACW: active channel width; RF: Random Forest; SVM: support vector machine; MRPP: multi-response permutation procedures

et al., 1974) and Green Red Vegetation Index (GRVI) (Tucker, 1979). Furthermore, the Normalized Difference Water Index (NDWI) (Gao, 1996) was calculated providing a measure of water content in soils and vegetation.

Beyond spectral indices, textural indices describe the distribution of grey tones in an image. This consists of a grey level co-occurrence matrix (GLCM) that interprets the spatial distribution of pairs separated by a certain distance in a given direction (Haralick et al., 1973). Seven texture metrics were selected in our study as candidate variables: variance, correlation, contrast, entropy, second moment, mean, and dissimilarity (Haralick et al., 1973). These metrics have been successfully applied by previous authors for vegetation, soil, crop and building classification (Leinenkugel et al., 2019; Zhang & Zhu, 2011).

3.1.2 | Sample points for machine learning

Classification of landforms in Mediterranean ephemeral rivers was carried out manually to construct a landform sample dataset for variable selection and supervised classification according to seven categories, and was based on the classification of Sanchis-Ibor et al. (2017), namely (1) channel and unvegetated gravel bar area (i.e., unvegetated gravel bars); (2) barely vegetated area, or deposits covered by grasses and scattered shrubs (< 5%); (3) mixed vegetated area covered by shrubs (< 50%) and scattered trees (< 5%); (4) fully vegetated area covered by shrubs (75%) and scattered trees (< 25%); (5) tree covered alluvial areas, covered by compact masses of trees in alluvial areas; (6) agricultural land; (7) water body, namely refers to reservoir and pond areas.

The sample points selection for the construction of the landforms dataset was carried out manually by visual photointerpretation. The 2019 aerial orthophoto available from the Institut Cartogràfic Valencià (ICV) (icv.gva.es/es) with a 0.25 m resolution on a 1:3000 scale was used. The sample points were extracted across the whole catchment and the result was a layer with 499 points with their associated landform class.

3.1.3 | Remote sensing variable selection

With a total of 16 variables calculated, the variable selection was carried out according to relative importance metrics in landform sample dataset. This step is required to obtain acceptable computational times and to reduce variable overlapping. We applied the Random Forest (RF) algorithm to rank variable importance in sample data using the Gini Impurity index (Breiman, 2001). RF is a machine learning algorithm based on tree decision rules (Breiman, 2001). The nodes are divided, in each decision tree, using a randomized subset of the variables. The final outcome is the majority votes from all trees. To obtain a consistent measure of the impurity of each variable we implement and additional k-fold cross-validation ($k = 3$) splitting the original sample into three (i.e., two training (66%) and one test (33%) datasets), repeated 10 times. This procedure generates 30 measurements of variable impurity. The aggregated median value of impurity was used to rank the variable importance. Additionally, RF requires hyperparameters optimization; for this reason, we performed a 10-fold repeated cross-validation and the number of predictors randomly selected in each tree decision (mtry) was 1–7, the minimum size of a node to be divided (min.node.size) was 2–30, and the number of trees value (ntree) was 500. This process was carried out with the CARET package (Kuhn, 2020) in R v. 3.3.3 software (R Core Team, 2019).

3.2 | River elements classification modelling

River elements classification was tested using two machine learning algorithms, support vector machine (SVM) and RF. RF algorithm was previously used to asses variable importance (Section 3.1.3.). In this section we use the results of the importance ranking of each variable to select the independent variables applied in the SVM and RF models. Radial SVM is a supervised machine learning technique that separates different categories by means of hyperplanes (Cortes & Vapnik, 1995).

Model training was the same for both algorithms. The sample point dataset was split into 80% for model training and 20% for testing model predictions. The best hyperparameters combination was tested using a more exhaustive cross-validation strategy, leave-one-out-cross-validation (LOOCV). This method is an iterative method that starts by using all available observations as a training set except one, which is excluded for validation. The process is repeated as many times as observations are available, excluding in each iteration a different observation, fitting the model with the rest and calculating the error with that observation. Finally, the error estimated by LOOCV is the average of all the calculated errors. SVM also requires hyperparameter optimization. In SVM, we optimized the gamma (defines how far the influence of a single training example reaches) and cost (trades off correct classification of training examples against maximization of the decision function's margin) hyperparameters with values spaced logarithmically between 0.001–1 and 1–700, respectively. For the SVM prediction we used a radial basis function kernel due to its high performance in land cover classifications (Thanh Noi & Kappas, 2018). For RF, using a linear spacing, the mtry parameter ranged from 1 to 3, the min. node.size from 2 to 30, and the ntree value was 500. To optimize hyperparameters and to model in both approaches we used the CARET package (Kuhn, 2020).

The supervised classification of river elements was validated using the testing subset. Additionally, we calculated the confusion matrix showing the performance of pixels with correct and incorrect predictions of the SVM and RF models. An accuracy index was obtained from the ratio of the correct predictions to the total number of pixels in the test dataset. Furthermore, we used the Kappa Cohen index (Cohen, 1960) when evaluating the classifiers' prediction performance.

3.3 | Geomorphic variables

Five geomorphic variables were used to characterize the Rambla de la Viuda stream network: active channel width, valley bottom width, slope gradient, route distance, and specific stream power (Table 1). All of these variables were extracted from a DEM with 25 m resolution from the 2009 Spanish National Plan for Aerial Orthophotography LiDAR (light, detection and ranging) project (PNOA-LiDAR Project) (https://www.cnig.es) resampled to 10 m using a bilinear interpolation method. All variables were estimated at 200 m intervals along the valley axis in a GIS environment (Alber & Piégay, 2011; Martínez-Fernández et al., 2016), using FLUVIALCORRIDOR 10.5 (Roux et al., 2015).

TABLE 1 Geomorphic variables used for achieving river segmentation by multi-response permutation procedures. The source and the methods applied for evaluating each variable every 200 m along the valley axis are also reported

Variable	Source	Description
Active channel width	Satellite image	Value automatically extracted from area covered by the channel and unvegetated gravel bar, barely vegetated area, and mixed vegetated area categories from the supervised classification (see Section 3.2.).
Valley bottom width	DEM	Polygon automatically extracted by using FLUVIALCORRIDOR 10.5 (Roux et al., 2015) and widths.
Route distance	DEM	Length of the stream inside the 200-m polygons.
Slope gradient	DEM	Calculated as the difference in stream channel slope between one point located 200 m upstream and another point located 200 m downstream and divided by the distance (i.e., 400 m).
Specific stream power	DEM, Satellite image	Calculation of $\omega = \gamma Qs/w$; where γ is the specific weight of water ($= 9800\ N/m^3$), Q is water discharge, s is energy slope (m/m) (Knighton, 1999) and w is the active channel width. Discharge (Q) value was obtained from the 'CAUMAX' data set associated with a 2-year flow event. Data available at www.miteco.gob.es.

DEM, digital elevation model.

3.4 | Methods for river segmentation

The detection of homogeneous river segments based on statistical methods has been developed extensively in the last few decades (e.g., Alber & Piégay, 2011; Brenden et al., 2008; Leviandier et al., 2012; Martínez-Fernández et al., 2016). These objective methods provide an alternative to expert judgement, as they are mainly based on visual and graphical estimations, and allow system discretization based on statistical criteria to be carried out. Compared to methods using only one variable (e.g., Guertault et al., 2018; Notebaert & Piégay, 2013; Parker et al., 2012), multivariate methods offer the possibility of simultaneously considering the complementary information provided by several variables (Bizzi & Lerner, 2012; Martínez-Fernández et al., 2019).

In the present work, multivariate analyses by multi-response permutation procedures (MRPP, Mielke, 1991) were performed to segment the studied fluvial network. MRPP are non-parametric techniques that allow the river network to be classified into internally

homogeneous and significantly different river segments. The null hypothesis states that equal probabilities are assigned to each of the possible allocations of the objects (reaches 200 m long, see Section 3.3.) into the groups (i.e., river segments). Hypothesis testing is based upon the MRPP statistic that quantifies the separation between groups by considering the objects in a Euclidian data space. This statistic is calculated as the weighted average of the within-group average Euclidean distance, indicating in the case of small values a tendency for clustering. The segmentation was done considering the five geomorphic variables shown in Table 1. First of all, a correlation test was applied to the five variables to detect redundancy among them (Pearson test, $p < 0.05$), with all correlations being less than|0.8|. All variables were standardized in each river before applying the algorithm and an alpha risk of 0.05 was considered to be statistically significant. For its application, MRPP was implemented using R (R Core Team, 2019). For more details about the procedure, see Martínez-Fernández et al. (2016).

3.5 | Channel type classification

After applying MRPP, each river segment was characterized by: (a) the average values of the geomorphic variables considered in the segmentation procedure, and (b) the average value of the landform classes extracted from the best performing model (Figure 2).

The five geomorphic variables were used to create homogenous groups after applying hierarchical cluster analysis (HCA). The Ward's linkage method (with squared Euclidean distance and *z*-score standardization) was used in this analysis. The range of variation of both geomorphic and landform variables (except 'water' class referring to reservoirs) were represented in boxplots and significant differences among typologies were assessed first by Kruskal–Wallis test, and, where significant differences existed, the differences were assessed by pairs using a Mann–Whitney Wilcoxon test (Wilcoxon, 1945). The functions *wilcox.test* and *hclust* of STATS package in R v. 3.3.3 software (R Core Team, 2019) were used to run the Wilcoxon test and the HCA, respectively.

4 | RESULTS

4.1 | Landform mapping using machine learning

Variable importance ranking for landform classification based on the RF analysis resulted in a selection of variables with a median higher than 80%, namely Blue, NDVI, Green and NDWI (see Supporting Information Figure S1). These selected variables include features of RGB, NIR and SWIR, avoiding the redundancy of bands. Texture indices are weak predictors in comparison with other variables as they have a relative importance median below 50%. The selected variables based on importance allow surfaces with or without vegetation to be differentiated.

Regarding river element classification, the hyperparameters used after optimization were gamma = 0.1 and cost = 100 in the case of SVM and, mtry = 3 and min.node.size = 30 in the case of RF. Visual inspection of the classification models shows a very similar pattern for both RF and SVM (Figure 3). The SVM method had an average accuracy and Cohen's Kappa values (Figure S2) of 0.87 and 0.84, respectively, which are similar to the RF model values of 0.85 and 0.81, respectively. The confusion matrix (see Supporting Information Table S1) shows that agricultural land is the class that contained the most misclassified pixels for both models. Based on these quantitative comparisons of the models' predictions, the SVM model was selected for the landform analysis. SVM shows the best performance, although all classes were predicted well by both models (Figure 3b,c). Among the classes, the best classification was obtained for the tree covered

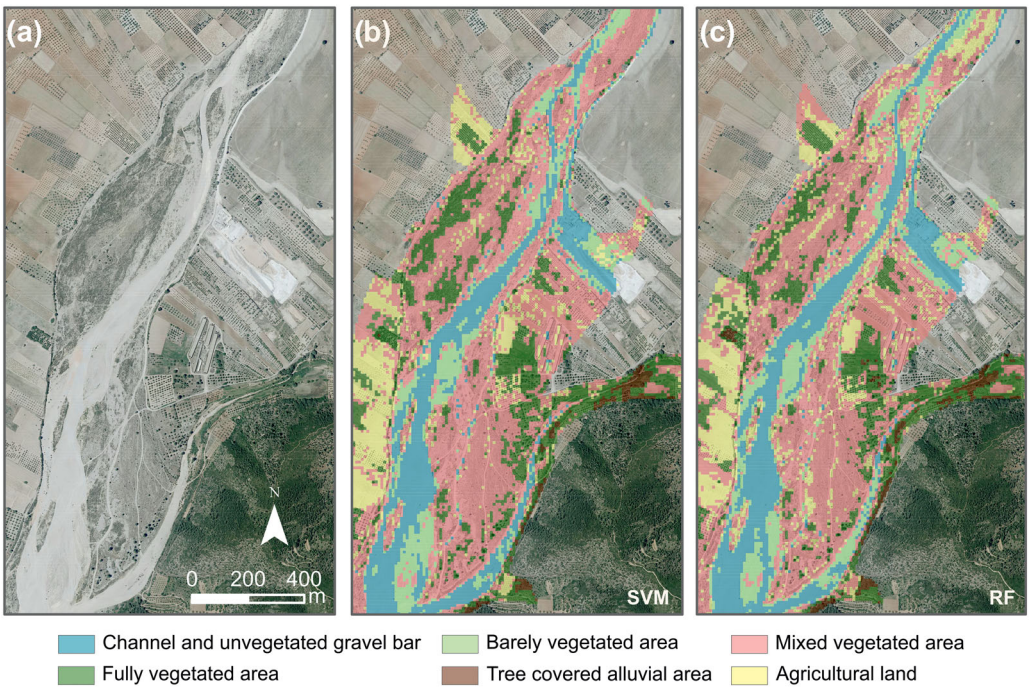

FIGURE 3 Subset of the classification results: (a) orthophotograph ICV 2019. (b) Support vector machine (SVM) prediction results. (c) Random Forest (RF) prediction results

alluvial area class. The prediction map (Figure 3) confirms that most misclassification occurred in the agricultural land class, which contained pixels misclassified as mixed vegetated or fully vegetated (Figures 3b and 4e). The channel and unvegetated gravel bar class was properly detected by the SVM method, which avoided any misclassification patterns or incorrectly classified pixels (Figure 4d,e).

4.2 | River segmentation using multivariate methods

A total of 62 segments were detected using the multivariate method (Figure 4a, see Table S2 for a complete description of the 62 segments). The average segment length is 4 km, with length reaches ranging between 0.6 km and 19.2 km in length. The highest number of segments was detected for the Rambla de la Viuda River corridor (36.8 km in total length), where 14 segments were detected with an average length of 2.6 km (Figures 4a and 5a,b), whereas only two segments were differentiated for the Riu Alcora (10 km in total length) with an average length of 5 km. Other streams (dels Olles, Benafigos and Solana) were considered as individual segments because significant differences along the stream were not detected using the multivariate method (Figure 4a).

Rambla de la Viuda contains the greatest diversity of segment types, and it serves to illustrate the relevance of the geomorphic variables in the segmentation process (Figure 4a). Figure 5(a) shows that the most relevant variables for segment detection are active channel and valley bottom width. Indeed, these variables show a similar pattern since a wider valley width allows for wider active channels. The longitudinal changes in these variables are controlled by structural and geological features. In particular, the boundary between graben and horst structures, which matches the transition from bedrock (limestones) to alluvial reaches, conditions the valley bottom width and, therefore, drives some of the major segment divisions. In segments with a narrow active channel, channel incision, observed in aerial photographs and field surveys, occurs in conjunction with high stream power values (see Figure 5b for an example of specific stream power peak in V2). Some break points are associated with morphological changes associated with anthropic structures, such as concrete channel lineaments, irrigation diversions, gravel mining (e.g., V7 to V8,

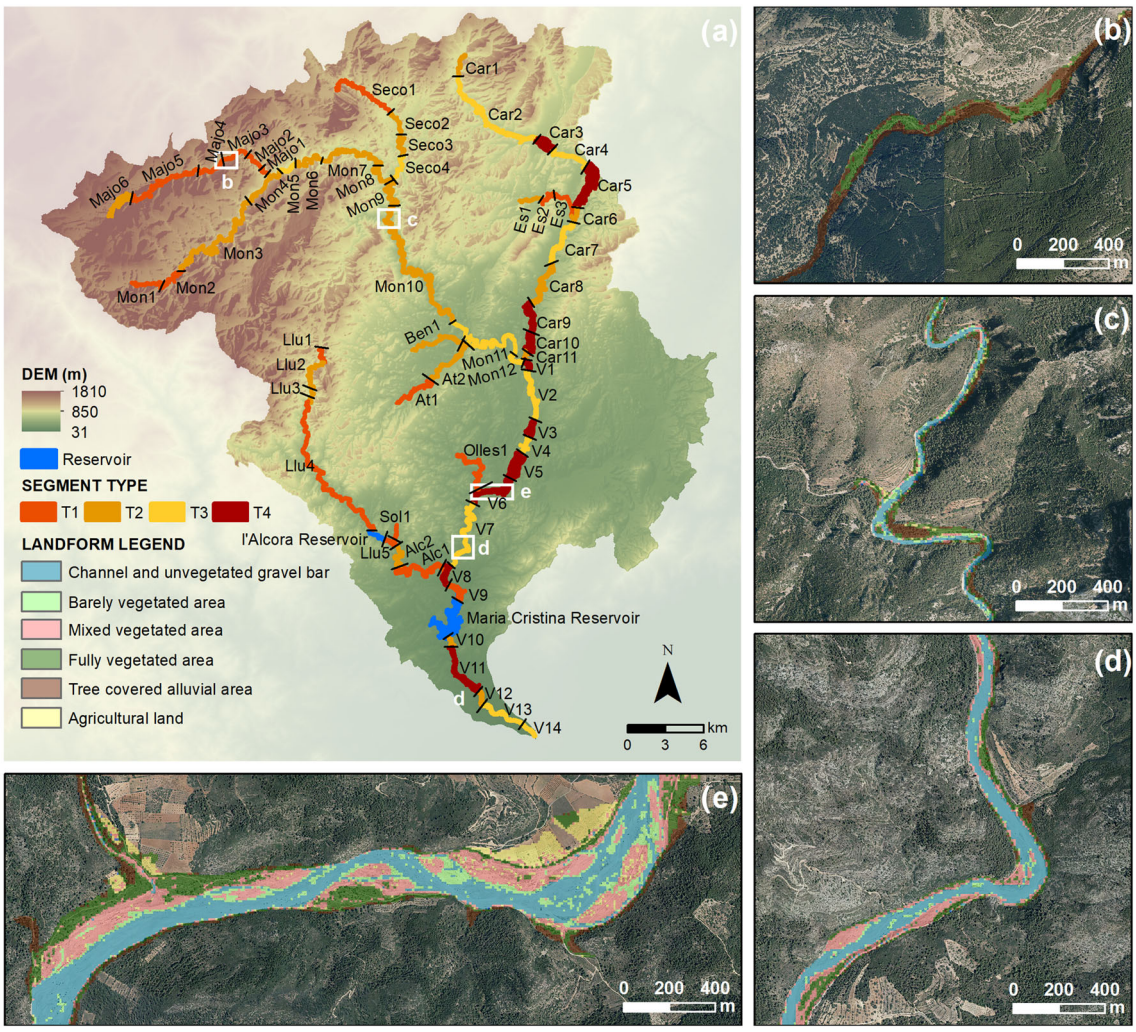

FIGURE 4 (a) The Rambla de la Viuda Basin and the delineation of river segments by channel types. (b) Subset of the supervised classification result for segment type 1. (c) Subset of the supervised classification result for segment type 2. (d) Subset of the supervised classification result for segment type 3. (e) Subset of the supervised classification result for segment type 4. Legend: Olles: Barranc de les Olles; Sol: Barranc de la Solana; At: Rambla de Atzeneta; Ben: Rambla de Benafigos; Car: Rambla Carbonera; Es: Rambla dels Estrets; V: Rambla de la Viuda; Majo: Majó River; Mon: Montlleó River; Seco: Seco River; Alc: Alcora River; Llu: Llucena River

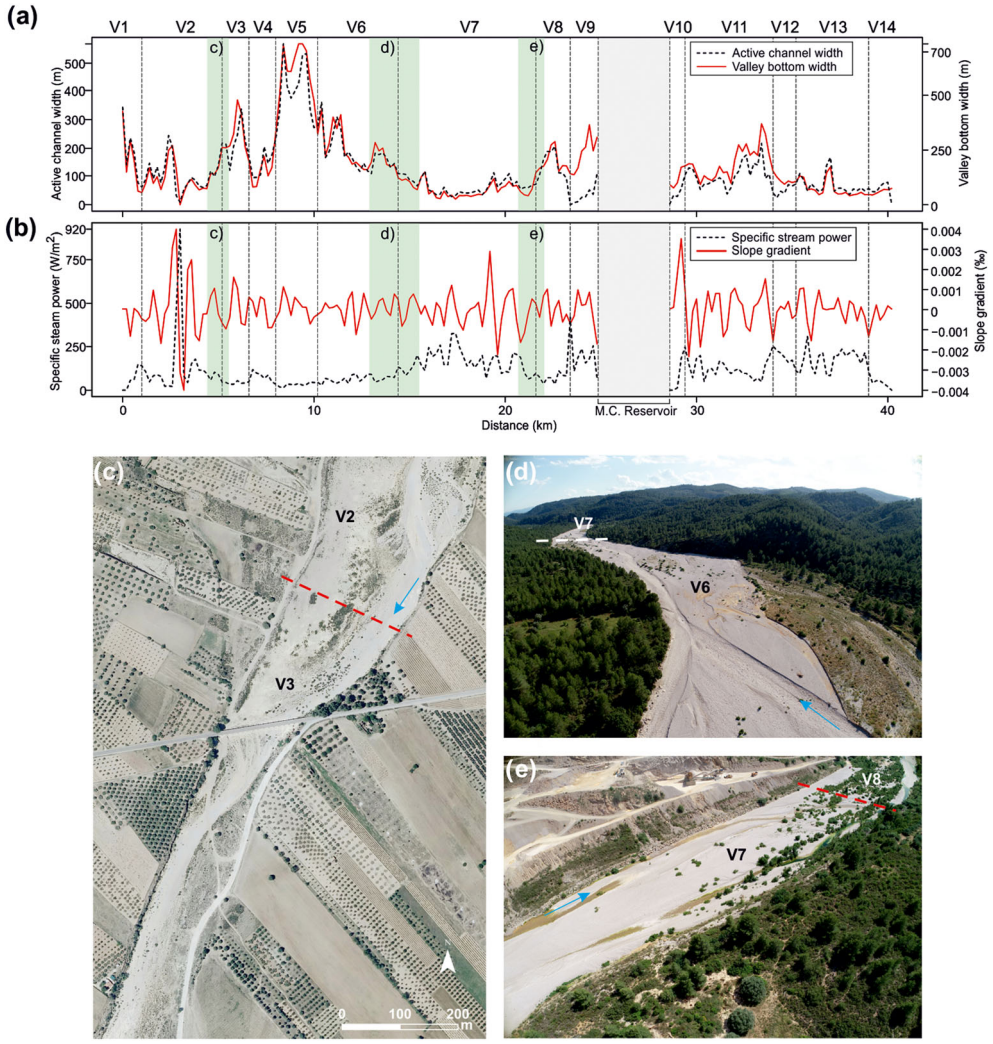

FIGURE 5 (a,b) Multivariate segmentation obtained with MRPP in Rambla de la Viuda. (c) Focus on channel narrowing between segment V2 and V3. (d) Focus on valley and channel narrowing between segments V6 and V7. (e) Focus on valley widening between segments V7 and V8. M.C. Reservoir: Maria Cristina Reservoir

Figure 5e), and dams (e.g., V10 to V11, Figure 5a). Slope gradient helps to distinguish between segments under dynamic equilibrium and those affected by erosion processes leading to channel incision. For example, V6 (Figure 5d), dominated by an alluvial active channel under dynamic equilibrium, contains only minor slope gradient changes, whereas V2 exhibits multiple channel bed steps in consolidated gravel giving rise to a high variability in slope gradient (Figure 5b,c). Interestingly, a sharp change in one single variable does not necessarily imply a segment break. For instance, the slope gradient peak in V7 occurred at a local channel step (related to in-channel gravel extraction) but within an overall gravel channel that does not result in a different segment. This result corroborates that the method is robustly multivariate, that is it does take change in several variables to prompt segmentation. The typological classification (Section 4.3.) will support that the segmentation process results in a robust and geomorphologically-meaningful segmentation method.

4.3 | Typological classification of segments

The analysis of the geomorphic parameters resulted in the differentiation of four main types of segments based on hierarchical cluster analysis (see Section 3.5., Figure S3). Results are shown as segment types T1 to T4 in Figure 4(a). T1 and T2 comprise the highest number of segments with 19 and 21, respectively, whereas T3 and T4 contain 12 and 10 segments, respectively (Table S3).

T1 is characterized by narrow active channels (14.7 m on average), significantly narrower than other groups (Willcoxon test, $p < 0.05$), within a narrow valley bottom (98.7 m on average), and with slope gradient and average specific stream power higher than other groups (Figure 6; Table S3). Channel and unvegetated gravel bars, barely vegetated area, and mixed vegetated area landforms show a significantly lower extent compared to other groups, whereas the relative extent of the fully vegetated area and, in particular, tree covered alluvial area were significantly higher than other groups (Figure 7). This group is mainly located in the headwaters in mountain areas and in bedrock confined valleys, which explains the frequent occurrence of relatively narrow channels occupied by mature vegetation (Figure 4a,b).

In T2, active channel width (32.9 m on average) is significantly wider than in T1 and significantly narrower than in T3 and T4 (Wilcoxon test, $p < 0.05$). Nevertheless, these channels are located within relatively narrow valleys (75.3 m width on average) (Figure 6; Table S3). Channel and unvegetated gravel bars extents are moderate, just as in T4. The proportion of mixed vegetated area is significantly larger than in T1 but lower than in T3 and T4 (Wilcoxon test, $p < 0.05$). The tree covered alluvial area class is lower than in T1 but still higher than in T3 and T4. The T2 segments are located in confined

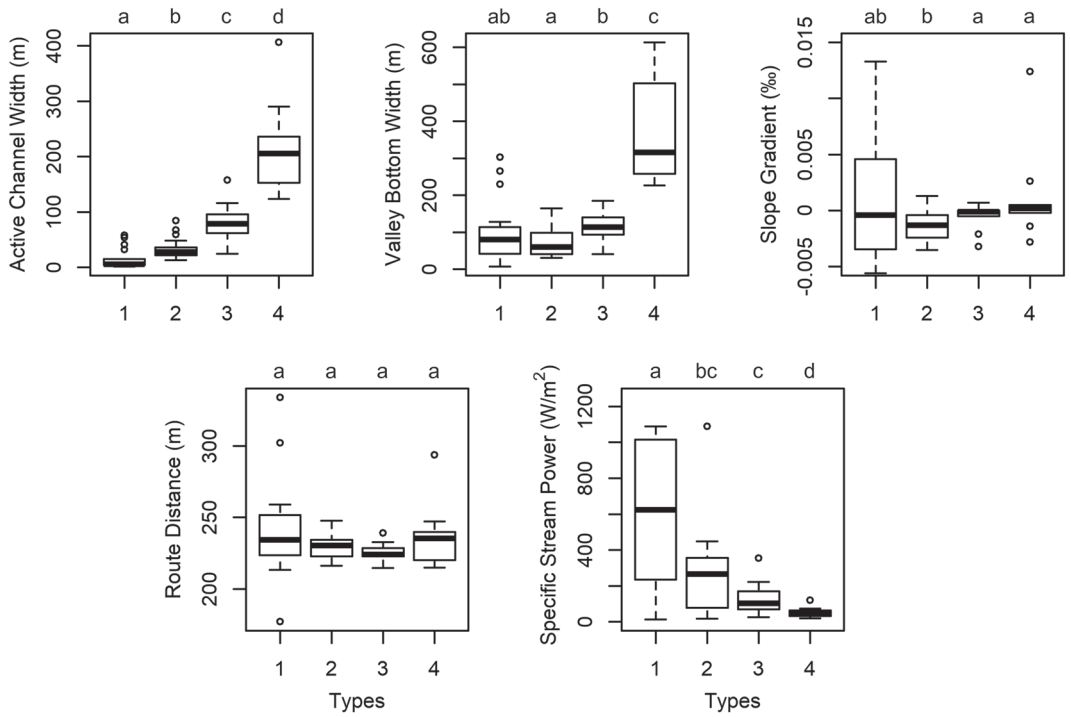

FIGURE 6 Distribution of the geomorphic variables of the four segment types. For each variable, different letters placed above each boxplot indicate significant differences among types of segments (Wilcoxon test, $p < 0.05$). For example, regarding active channel width, the four different letters mean that the four types are significantly different between them

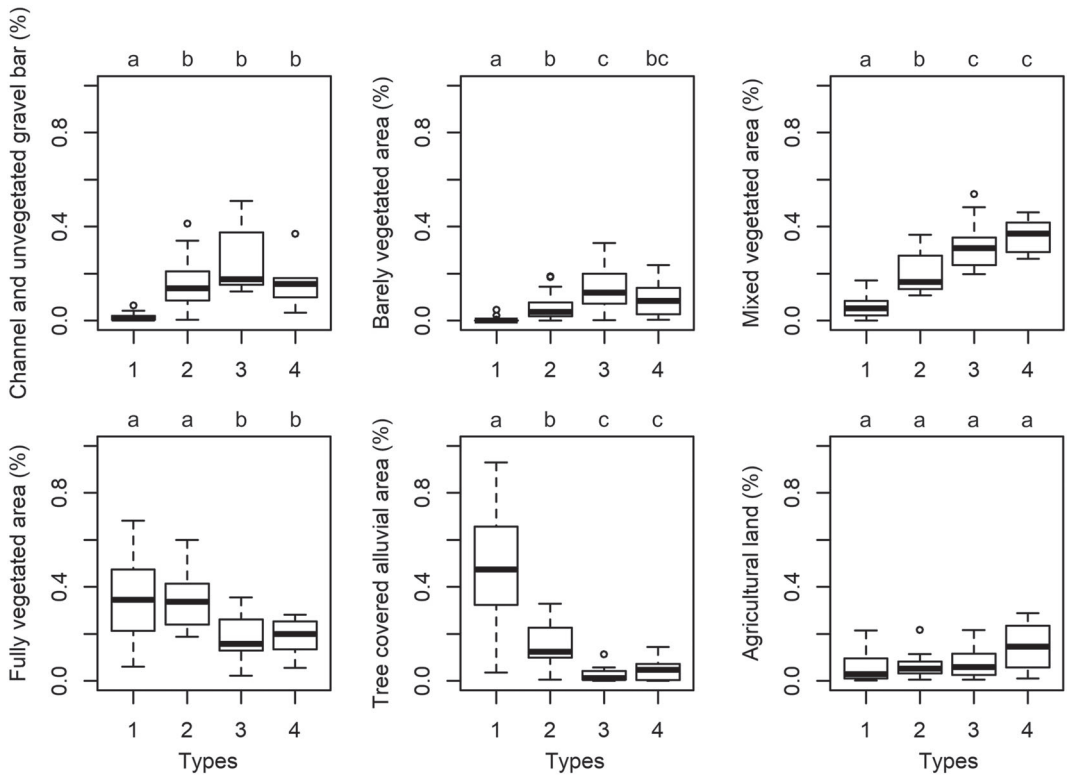

FIGURE 7 Distribution of the landform variables of the four segment types. For each variable, different letters placed above each boxplot indicate significant differences among types of segments (Wilcoxon test, $p < 0.05$). For example, regarding fully vegetated area, type 1 and type 2 are significantly different from type 3 and type 4

bedrock valley sides in the mountain sectors with broader active channels and mixed vegetation on gravel bars (Figures 4a,c and 7).

T3 comprises an intermediate channel width (80.6 m on average) within moderately open valleys (113 m on average), significantly wider than in T1 and T2 and narrower than in T4 (Figure 6). T3 contains the highest proportion of channel and unvegetated gravel bar and barely vegetated landforms (significantly so in relation to the latter after a Wilcoxon test, $p < 0.05$). The proportions of the fully vegetated area

and tree covered alluvial area are significantly lower than in T1 and T2. In T3, the segments contain a well delineated and continuous active channel partly laterally confined within mixed bedrock-alluvial valleys (Figures 4d and 7).

Finally, T4 is characterized by a significantly wider active channel and valley bottom (Wilcoxon test, $p < 0.05$) than other groups, namely of 217.3 m and 369.7 m width on average, respectively, leading to the lowest values for specific stream power (Figure 6). In T4 the proportion of channel and unvegetated gravel bar extents are similar to in T2 and T3. However, T4 shows relatively wide and continuous channels, with a higher extent of mixed vegetated area and agricultural land due to their location on wide alluvial valley bottoms (Figures 4e and 7).

5 | DISCUSSION

Our methodological approach for ephemeral stream classification combines two independent quantitative geomorphologic analyses and provides two distinct advantages: (1) the use of objective criteria with a replicable methodology to define stream channel types, and (2) the automatic analysis of the spatial distribution of each channel type and associated landform classes covering extensive river networks (i.e., catchment and regional scales). Herein, we firstly evaluate the robustness of our landform class mapping approach given the Sentinel-2 image resolution and algorithms used on landform class mapping (Section 5.1.). Second, the significance of the river segmentation and stream supervised classification in the context of previous stream classifications and other machine learning examples is discussed (Section 5.2.). The relation of typologies to the disturbance regime is then reviewed (Section 5.3.) followed by the potential of automatic stream classifications for a first-order approximation tool in river environmental protocols for managers (Section 5.4.).

5.1 | Landform class mapping challenges

Our approach, which combines remote sensing and machine learning techniques, provides objective and semi-automatic fluvial landform mapping for Mediterranean ephemeral streams. Recent advances in geomorphologic mapping and spatial classification of rivers are based on aerial images (Gilvear et al., 2004), high-resolution aerial images (Carbonneau et al., 2020; Rivas Casado et al., 2015, 2017), very high resolution (VHR) or VHR near-infrared aerial imagery combined with topography (Demarchi et al., 2016, 2017, 2020), and satellite images combining DEM and orthophotos (Spada et al., 2018). Despite the noteworthy methodological progress achieved, detailed mapping of fluvial landforms (e.g., bars, island, pools) in medium sized rivers (20–200 m wide) is still challenging given the low spatial resolution of open-source satellite images and algorithms for attribution of landform classes. Recent studies improved their resolution using VHR RGB images to identify riverscape units at the catchment (Demarchi et al., 2016) and even the continental scale (e.g., Europe; Demarchi et al., 2020). However, using VHR images to this extent increases the computational time but also results in an excessive amount of information that requires a simplification process to portray fluvial units at the map scale. We propose the use of Sentinel-2 satellite images because of their 12 spectral bands and great potential for diachronical analysis covering specific dates, which is crucial for documenting flood disturbance and human pressures. Moreover, Sentinel-2 images require a relatively low computational load, which in this case was achieved using Intel Iris Plus Graphics, 16GB RAM and Intel Core i7-1065G7 CPU wherein the processing time is 30 min for ranking variable selection and 120 min for completing the machine learning algorithms. Despite its limited resolution (10 m), which hinders its application in narrow streams, the worldwide availability of Sentinel-2 images makes our approach extendable to basically any river and, in particular, to IRES.

Remote sensing has also benefited from technical developments in big data analysis. In our study, machine learning algorithms (SVM and RF) were applied to obtain a spatial classification. Using the same combination of single spectral bands and indices in both methods, we obtained accuracies and kappa values higher than 80%, with the best accuracies obtained with the SVM method as shown in previous studies (e.g., Phiri et al., 2020). These accuracies are similar to those achieved by McManamay et al. (2018) using RF and slightly higher than the 72% obtained by Beechie and Imaki (2014) with SVM for predicting channel patterns using hydro-sedimentary and topographic variables. One of the major challenges was distinguishing agricultural lands from the mixed vegetated areas on the floodplain. These land classes may give similar spectral characteristics due to the fact that agricultural land is principally composed of scattered fruit trees with grass in this region, and grain fields that resemble grassland fields after harvesting. Demarchi et al. (2020) differentiated sediment bars from bare soil fields using RGB spectral bands but encountered similar problems in separating vegetation cover classes. In our study, we use a near-infrared spectral band to differentiate the different types of vegetation. The combination of spectral information with a topographic layer proved to be a satisfactory solution (Demarchi et al., 2016), with the near-infrared band being essential for differentiating vegetation. Still, remote sensing derived fluvial landform mapping is highly dependent on vegetation type and density, meaning that compound bars (e.g., lateral bars with lobate sediment units) and channel mesoforms (e.g., pool-riffles) formed during the same disruptive event are seldom differentiated. Future research should include topographic information to improve the identification of (i) compound fluvial mesoforms and (ii) to solve the confusion between landform classes such as the distinction between mixed vegetated area and agricultural land.

5.2 | Segmenting and establishing types for ephemeral channels

River segmentation from multivariate analysis combined with the classification of six landform units from remote sensing has resulted in the channel network being classified into four types. This channel network classification based on automatic river segmentation and remote sensing (RS) contains features of three previous geomorphic classifications that describe: (1) longitudinal stream zonation within drainage basins, namely erosion, transport and deposition zones (Bull, 1979; Schumm, 1977; Sutfin et al., 2014); (2) fluvial landform assemblages (Montgomery & Buffington, 1997; Rosgen, 1994); and (3) process domains (Montgomery, 1999; Whiting & Bradley, 1993). The spatial data analysis combines geomorphological and vegetation attributes,

providing three main advantages. Firstly, the multivariate segmentation solves the difficulty of objectively identifying channel types along bedrock-alluvial transitional states through analysis of DEM data. This segmentation procedure identifies segment boundaries derived from changes in geometric and hydraulic variables that otherwise would not be straightforward from a visual or field interpretation, particularly in transitional reaches (Sutfin et al., 2014). Secondly, segment-level landform units were mapped using machine learning algorithms on satellite images, which offers uniformity and consistency in the mapping criteria. This technique enables very efficient application to large areas with moderate effort, even in those areas located in remote sites that are difficult to access, as long as a satellite image is available. Thirdly, the statistical cluster analysis of geomorphologic assemblages at the segment scale provides a suite of process domain attributes for segment affinity among channel morphological types. Different statistical approaches for hierarchical clustering have been used in fluvial geomorphology, including the Ward's method applied in this study (Clubb et al., 2019; Henshaw et al., 2020), and multivariable k-means statistical clustering (Dallaire et al., 2019; Thoms et al., 2018). The k-means cluster approach provides a simple set of clusters without a particular structure within them whereas Ward's method finds a large set of clusters which are merged in the process based on their affinity (Ward, 1963). Ward's method is the most widely used algorithm for identifying landscape units, and differs from other methods in that it uses an analysis of variance approach to determine distances between clusters. In general, this method is very efficient, as it allows the distances between clusters to be evaluated from an analysis of the variance (Zhang et al., 2017).

The variables involved in the cluster analysis include both RS derived landform units and topographic/hydraulic variables inherently connected by fluvial processes. Commonly, these process domains (Montgomery, 1999) are associated with landscape controls idealized as a downstream progression from source (headwater: bedrock-control), transport (piedmont: mixed bedrock-alluvium) and response reaches (low lands: alluvial streams), analogous to those described by Sutfin et al. (2014). In our case, the spatial variability of landforms and process domains are complex due to geologic and structural controls (i.e., horst and graben zones). Bedrock type and topography strongly influence the in-channel landform structure and variability (Grant & Swanson, 1995) in response to the dominant process and capacity for geomorphic adjustment (Fryirs & Brierley, 2010). This classification approach therefore reflects fundamental differences along the river channel network and recognizes disruptions of the river continuum of a morpho-sedimentary character along a gradation of stream power (Bridge, 1993) and confinement (Sutfin et al., 2014) trends.

The spatial distribution of channel types can be explained by differences in geometric (i.e., active channel/valley bottom width, and slope gradient) and hydraulic (i.e., specific stream power) parameters. The alluvial landforms' (mainly classified by vegetation cover) distribution and extent depend on erosion and deposition spots during flow runs and on the time since the large disruptive flood event. There is a general spatial trend from headwater to lowland in the distribution of channel types, namely from T1 to T4 (Figure 8). Headwater segments (i.e., T1 and T2) are characterized by confined valleys that allow direct sediment input via hillslope processes. Colluvial channels, within source areas dominated by gravity flows, were not identified at the satellite image scale. In T1 segments, the specific stream power is very high but the abundance of tree covered alluvial area is likely related to the episodic rate of sediment supply (Figure 8). The wide range in specific stream power and slope gradient found in these segments agrees with dominant alluvial morphology found in cascade and step-pool sequences. Low percentages of barely vegetated and mixed vegetated areas in T1 suggest that these channel segments are highly resilient to morphological change likely due to their connection with reaches characterized by limited or lack of sediment supply, according to the degrees of connectivity proposed by Hooke (2003).

Along with T1, T2 is predominant in headwaters that possess a medium degree of confinement and a little variability in slope gradient (Figure 8). The channel and unvegetated gravel bar are well delineated, with some discontinuities, as are the mixed vegetated areas likely associated with increasing activity of alluvial morphogenetic processes. The lower variability in specific stream power and in slope gradient corroborates the alluvial morphologies dominated by pool-riffle and plane-bed sequences. The confined channels and pool-riffle morphologies may imply increasing sediment supply and sustained

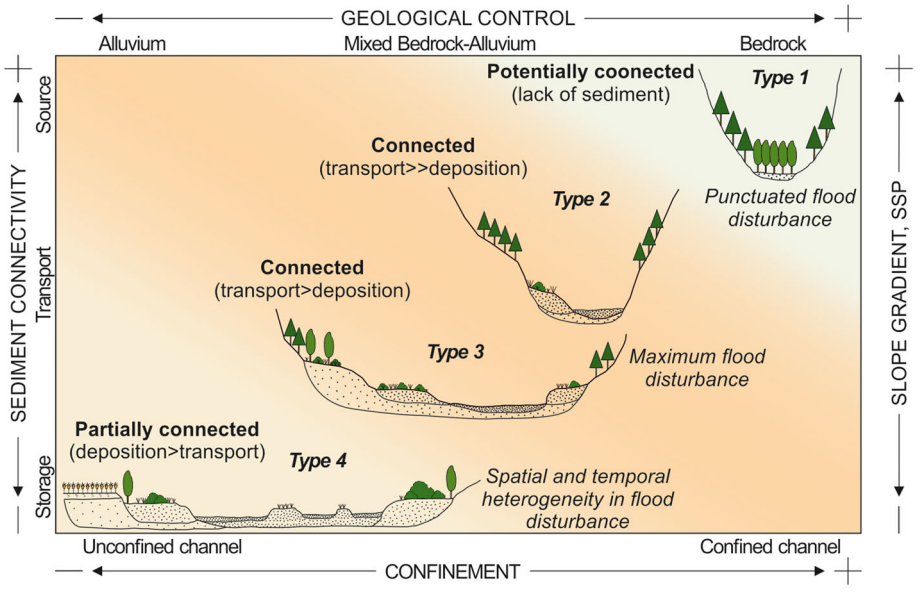

FIGURE 8 Schematic illustration of channel types' cross-sections relative to different valley/segment geometric and geomorphological characteristics. A qualitative evaluation of the longitudinal sediment connectivity according to Hooke (2003) classes is indicated. The background colour refers to the degree of natural disturbance by flooding inferred from spatial position within the catchment and the flood power relative to the channel width (darker being higher). Legend: SSP: specific stream power; +: maximum; −: minimum

particle transport conditions (Papangelakis & Hassan, 2016). T2 segments show functional geomorphic characteristics compatible with a seasonal flow that efficiently conveys sediment load producing significant geomorphological adjustments (Montgomery & Buffington, 1997). This channel type is morphologically resilient to textural and geometric changes (Fryirs & Brierley, 2016) with increased sediment connectivity during peaks of gully and hillslopes material input.

T3 segments comprise mixed alluvial-bedrock channels whose spatial distribution is controlled by geologic and structural conditions (Figure 8). The active channel, significantly wider than in T1 and T2, shows a continuous trace along narrow valleys entrenched on bedrock or consolidated alluvium. The fluvial landforms consist of transverse and lateral gravel bars dominated by unvegetated to barely vegetated covers, suggesting significant morphological adjustments during episodic flooding. The lower variability of specific stream power and slope gradient indicates sustained transport capacity and sediment connectivity during normal flow events. These reaches show a high sensitivity to upstream changes in sediment supply related to extreme events or human activity. In this regard, these segments are ideal locations to monitor channel response and recover potential on the watershed scale.

T4 segments occur at alluvial depressions with a high valley bottom width. These segments comprise wide active channels with low specific stream power and slope gradient values (Figure 8). The channel morphology consists of longitudinal, transverse and lateral gravel bars characteristic of depositional zones (Montgomery & Buffington, 1997; Schumm, 1977). The highest percentage of mixed vegetated areas is characteristic of multithread channels that shift, producing local erosion and deposition (Schumm, 1977). In general terms, segments of T4 are competence-limited channels (lowest specific stream power values, Figure 6), which implies only a partial connection to the stored sediment.

5.3 | Linking reach-level landform classes and disturbance regime

A challenge in watershed-based classifications is the spatial–temporal geomorphic adjustment of river landforms to either natural or anthropic geomorphic disturbances (Fryirs & Brierley, 2016). In ephemeral streams, most geomorphic effective work (i.e., sediment transport and landform changes) is performed by large flood events (Tooth, 2000). Indeed, the distribution of vegetation species across the landforms is governed by the tolerance and exposure of species to flood disturbance and water stress regimes (Hupp & Osterkamp, 1996; Manning et al., 2020). According to Montgomery (1999), a watershed may be divided into spatially identifiable areas, or process domains, along the river network, dominated by distinctive geomorphic processes, disturbance regimes, and response potential. The landform and vegetation structure of segment types provides insight into the processes resulting from the disturbance regime and their physical impacts (Figure 8). For instance, disturbance by floods is enhanced in confined channels in comparison to unconfined channels (Gregory et al., 1991). The landform distribution analysis confirms that the partially confined streams in T3 comprise the highest unvegetated and barely vegetated landform areas, likely associated with frequent vegetation reset by flooding (Hupp & Osterkamp, 1996; Sanchis-Ibor et al, 2017). The greatest percentage of mixed vegetated bars in T4 segments suggests the importance of a localized erosion and deposition processes in wider unconfined channels (Figure 7). In this comparison, a lower percentage of barely vegetated bars in T4 segments indicates more resilient conditions or a capacity to absorb changes in water and sediment discharge without significant morphological response (Poff et al., 1997).

Future alternatives of the proposed approach could incorporate a spatio-temporal dimension to the process-based analysis by considering satellite images of multiple years or months (or even weeks depending on availability) allowing the assessment of single extraordinary events such as the disturbance generated by a flood or the alteration caused by a human impact such as a weir construction. Moreover, the future availability of satellite images with higher resolution would facilitate a more detailed classification of landforms and mesoforms, together with a better characterization of several types of artificial interventions (i.e., artificial levees, dykes, lining works, transversal and crossing structures, etc.). As geospatial data are evolving fast to provide new products with higher resolution and shorter acquisition time intervals these shortcomings for the hydromorphological assessment at reach scale will be reduced.

5.4 | Towards an environmental assessment tool in ephemeral channels

The size, shape, and character of a river channel reflects components of prevailing flow and sediment bedload (Leopold et al., 1964). Thus, any change in sediment and water fluxes, occurring either naturally or as a result of human activity, implies an adjustment of the channel to new equilibrium conditions (Downs & Gregory, 2004; Kondolf, 1995). The proposed stream classification does not inherently aim to guide geomorphic recovery, but it may offer a first-cut analysis to help identify and evaluate degraded segments based on anomalous morpho-sedimentary patterns. Open geospatial data currently available for most countries (Sentinel-2 images, LiDAR data) and GIS resources make the proposed approach suitable for regional scale baseline surveys of reach types and river landscape units. Based on the spatial configuration of morphological characteristics and stream types, it is possible to identify dominant river processes (entrenchment, sediment continuity, bank erosion, etc.) and their relation to human impacts and disturbances.

As an example, we select an obvious example of the impacts of transversal barriers such as dams on the measured morpho-sedimentary parameters and river type spatial configuration within the studied catchment. The morpho-sedimentary impacts at the Maria Cristina Reservoir (Figure 1) is patent in the upstream segment but also downstream. At the tail of this reservoir, channel slope decreases along with a reduction on sediment delivery and morphologic activity enhancing vegetation growth (segment V9 of T1; Figure 9a). Note that this T1 segment, typical of headwater zones, with a low channel slope and located next to the dam, is itself anomalous. Downstream from the dam wall, the location of stream channels T1 and T2 with narrow active channels and anomalous slopes suggests a sediment transport decay, which leads to adjustments in channel geometry (Figure 9a,b). The most degraded

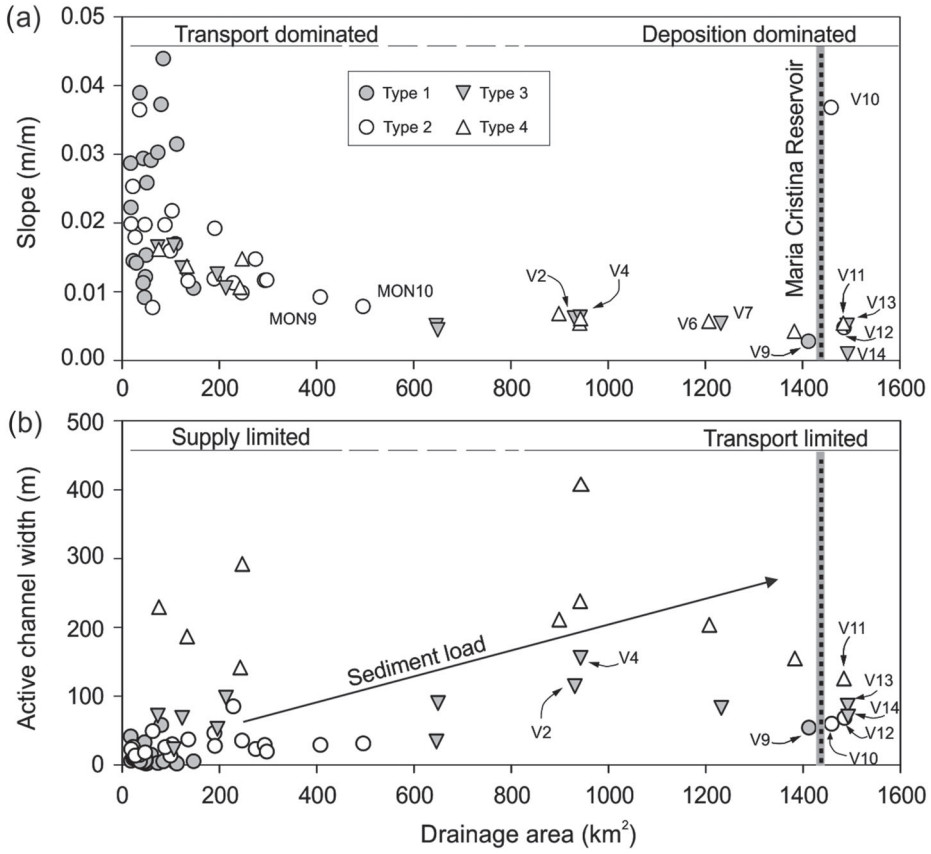

FIGURE 9 Diagrams of watershed, topographic variables and stream type classification. (a) Drainage area versus channel slope for the identified segments with indication of the classification type. (b) Drainage area versus active channel width. The arrow illustrates the generalized relative trend in sediment load broken at the Maria Cristina dam barrier. Numbers of segments refer to Figure 5

reaches occur in a short reach below the dam (V10 to V12) with a reduction of ~50% in channel width in comparison to segments located upstream of the dam (Figure 9b). River adjustments continue downstream to the T4 (V11) and T3 (V13 and V14) segments, causing a reduction of active channel width and slope (Figure 9a,b). Morphological changes in channel width are distinctive of reservoir impacts worldwide, with cases where channel width decreased by 90% or increased by as much as 100% (Downs & Gregory, 2004; Williams & Wolman, 1984). These observed geomorphic alterations therefore indicate a change in the sedimentary continuity and connectivity at this point (Fryirs, 2013; Wohl, 2017). Since sediment load-carrying capacity is proportional to the alluvial width, bed slope and discharge (Martín-Vide et al., 2020), the observed decrease in active channel width (Figure 9b) indicates a reduction in sediment load, which, under natural conditions, should tend to increase downstream (Mueller & Pitlick, 2005; Pitlick et al., 2008).

Downstream of the Alcora Reservoir (Figure 4a), long segments of full vegetated channels (T1) are interpreted to result from a significant reduction in floods and sediment fluxes from the dam. This reduction of channel capacity (section area and slope) downstream of the Alcora dam persists for ~11.4 km until the junction with the Rambla de la Viuda stream where the increase in contributing catchment area partially mitigates for the influence of the dam on sediment and water flows (Gregory & Park, 1974).

Other segments suggesting sediment discontinuity are associated with in-stream gravel mining. In particular, V12 (T2) and V4 (T3) show narrowing and discontinuity of the active channel assumed to be related to channel incision caused by aggregate mining, based on evidence from field surveys and reach-scale photogrammetric mapping (Calle et al., 2017; Calle et al., 2020). Other effects of mining activity include the formation of knickpoints that eventually may migrate several kilometres upstream during flooding (Kondolf, 1994). Field evidence of repeated knickpoints within a single segment is potentially detected by our spatial analysis from anomalous values of slope gradient at specific segments (e.g., V2, V7, V10; Figure 5b).

6 | CONCLUSIONS

An essential first step in the analysis of IRES status is to classify channel types representing the spatial diversity of geomorphic processes and their dynamic interaction with vegetation. In this study, we present an objective, semi-automatic and replicable approach for the segmentation and classification of channels with similar morphology using (1) automatic segmentation procedures using GIS tools and statistical methods and (2) reach-scale landform classes using machine learning algorithms applied to satellite images. Four channel types were defined from a cluster analysis of 62 segments of the Rambla de la Viuda catchment (1500 km^2), with the typology based on differences in elements of the valley/channel geometry, fluvial landform assemblage, and hydraulic conditions. Segments T1 occurs on narrowly confined segments in headwater areas with a high stream gradient, reduced riparian zones, and boulder dominated bedforms (cascade or step-pool channels). Segments T2 occurs in partly confined segments in piedmont sectors with a high-moderate gradient, narrow riparian zones, and discontinuous bed gravel landforms (plane bed to step-pool). Segments T3 comprises semiconfined reaches in lowlands with a moderate gradient, broader riparian zones, and continuous bed gravel landforms (lateral gravel bars). Finally, segments T4 consists of unconfined segments with a low channel gradient, well-developed riparian zones, and wide continuous active gravel bed landforms (multithread channels).

The applied catchment-scale stream analysis and channel classification is an efficient tool for: (1) understanding the geological, structural, and vegetation controls on the spatial distribution of channel morphology; (2) interpreting fundamental processes (depositional and erosional) and disturbance regimes at the reach scale through links between alluvial landforms and vegetation density; (3) identifying the location of reaches that supply and store sediments; (4) predicting, based on the former, the sediment continuity through the river network; and (5) identifying geomorphic disequilibrium and its causal links with natural and anthropogenic impacts.

The applied methodology is particularly well-suited for ephemeral streams whose environmental quality assessment depends on geomorphological conditions that support riparian habitats. It is important to recognize that channel categories and the distribution of geomorphic processes (process domains) depend upon internal controls (e.g., climate, geology and topography), therefore, the classification presented here is not intended to be universal in its channel types but in its methodological approach. A fundamental advantage of this approach is the objective delineation of stream segments along a continuous river network, which enables systematic characterization of extensive Mediterranean regions. Currently, a limiting factor in fluvial landform delineation is the spatial resolution of the available open-access satellite imagery, but it is likely that this drawback will be overcome by new products released by space agencies (e.g., ESA, NASA). Automated approaches that are applicable over large regions lay the foundations for an essential characterization of river channels, including their management, conservation and restoration of river corridors. In particular, the application in IRES is highly appropriated because of the lack of summer flows, which leaves the bed exposed, and the limited riparian canopy relative to perennial river channels.

ACKNOWLEDGEMENTS

The research conducted in this study was funded by the Ministry of Science and Innovation through the projects EPHIMED (CGL2017-86839-C3-1-R) and EPHIDREAMS (PID2020-116537RB-I00), co-financed with FEDER funds. M.P. Rabanaque and V. Martínez-Fernández were funded by Spanish Ministry of Science and Innovation contracts, namely from the PhD FPI programme (PRE2018-086771) and Post-doc Juan de la Cierva programme (FJC2018-035451-I) respectively. M.C. was partly financed by the EPHIMED project, Turku Collegium of Science, Medicine and Technology (TCSMT) and Hydro-RDI-Network, Academy of Finland funding ID: 337279. This work is part of CSIC-PTI TELEDETECT activity. This article is a contribution of the Hydrology and Climate Change Laboratory (www.floodsresearch.com; twitter: floods_research; instragram: @floods_research). The authors finally thank the editor and the two reviewers for their helpful suggestions.

CONFLICT OF INTEREST

The authors declare that they have no know competing financial interests or personal relationships that could have appeared to influence the work reported in this paper.

DATA AVAILABILITY STATEMENT

The data that support the findings of this study are available from the corresponding author, upon reasonable request.

ORCID

Maria Pilar Rabanaque https://orcid.org/0000-0002-6551-9351
Vanesa Martínez-Fernández https://orcid.org/0000-0003-0922-4134
Mikel Calle https://orcid.org/0000-0003-1590-6772
Gerardo Benito https://orcid.org/0000-0003-0724-1790

REFERENCES

Alber, A. & Piégay, H. (2011) Spatial disaggregation and aggregation procedures for characterizing fluvial features at the network-scale: Application to the Rhône basin (France). *Geomorphology*, 125, 343–360. https://doi.org/10.1016/j.geomorph.2010.09.009

Anadón, P. & Moissenet, E. (1996) Neogene basins in the Eastern Iberian Range. In: Dabrio, C.J. & Friend, P.F. (Eds.) *Tertiary Basins of Spain: The Stratigraphic Record of Crustal Kinematics*. Cambridge: Cambridge University Press, pp. 68–76.

Beechie, T. & Imaki, H. (2014) Predicting natural channel patterns based on landscape and geomorphic controls in the Columbia River basin, USA. *Water Resources Research*, 50, 39–57. https://doi.org/10.1002/2013WR013629

Beneyto, C., Aranda, J.Á., Benito, G. & Francés, F. (2020) New approach to estimate extreme flooding using continuous synthetic simulation supported by regional precipitation and non-systematic flood data. *Water*, 12, 1–16. https://doi.org/10.3390/w12113174

Benito, G., Sanchez-Moya, Y., Medialdea, A., Barriendos, M., Calle, M., Rico, M. et al. (2020) Extreme floods in small mediterranean catchments: Long-term response to climate variability and change. *Water*, 12, 1–23. https://doi.org/10.3390/W12041008

Bizzi, S. & Lerner, D.N. (2012) Characterizing physical habitats in rivers using map-derived drivers of fluvial geomorphic processes. *Geomorphology*, 169–170, 64–73. https://doi.org/10.1016/j.geomorph.2012.04.009

Borak, J.S. (1999) Feature selection and land cover classification of a MODIS-like data set for a semiarid environment. *International Journal of Remote Sensing*, 20, 919–938. https://doi.org/10.1080/014311699212993

Breiman, L. (2001) Random Forests. *Machine Learning*, 45, 5–32. https://doi.org/10.1023/A:1010933404324

Brenden, T.O., Wang, L., Seelbach, P.W., Clark, R.D., Wiley, M.J. & Sparks-Jackson, B.L. (2008) A spatially constrained clustering program for river valley segment delineation from GIS digital river networks. *Environmental Modelling & Software*, 23, 638–649. https://doi.org/10.1016/j.envsoft.2007.09.004

Bridge, J.S. (1993) The interaction between channel geometry, water flow, sediment transport and deposition in braided rivers. In: Best, J.L. & Bristow, C. (Eds.) *Braided Rivers: Form, Process and Economic Applications*, Geological Society, Special Publication 75. London: The Geological Society, pp. 13–71.

Brierley, G.J. & Fryirs, K.A. (2005) *Geomorphology and river management: Applications of the river styles framework*. Oxford: Blackwell Publishing.

Bull, W.B. (1979) Threshold of critical power in streams. *GSA Bulletin*, 90, 453–464. https://doi.org/10.1130/0016-7606(1979)90<453:tocpis>2.0.co;2

Calle, M., Alho, P. & Benito, G. (2017) Channel dynamics and geomorphic resilience in an ephemeral Mediterranean river affected by gravel mining. *Geomorphology*, 285, 333–346. https://doi.org/10.1016/j.geomorph.2017.02.026

Calle, M., Calle, J., Alho, P. & Benito, G. (2020) Inferring sediment transfers and functional connectivity of rivers from repeat topographic surveys. *Earth Surface Processes and Landforms*, 45, 681–693. https://doi.org/10.1002/esp.4765

Camarasa, A.M. & Segura, F. (2001) Flood events in Mediterranean ephemeral streams (ramblas) in Valencia region, Spain. *Catena*, 45, 229–249. https://doi.org/10.1016/S0341-8162(01)00146-1

Carbonneau, P.E., Dugdale, S.J., Breckon, T.P., Dietrich, J.T., Fonstad, M.A., Miyamoto, H. & Woodget, A.S. (2020) Adopting deep learning methods for airborne RGB fluvial scene classification. *Remote Sensing*

of Environment, 251, 112107. https://doi.org/10.1016/j.rse.2020.112107

CHJ (Confederación Hidrográfica del Júcar) (2018) Evaluación del estado hidrogeomorfológico en los ríos efímeros de la Confederación Hidrográfica del Júcar. Informe FP.OPH.002/2017. Valencia: CHJ, 266 pp.

Clubb, F.J., Bookhagen, B. & Rheinwalt, A. (2019) Clustering river profiles to classify geomorphic domains. *Journal of Geophysical Research: Earth Surface*, 124, 1417–1439. https://doi.org/10.1029/2019JF005025

Cohen, J. (1960) A coefficient of agreement for nominal scales. *Educational and Psychological Measurement*, 20, 37–46. https://doi.org/10.1177/001316446002000104

Cooke, R.U. & Doornkamp, J.C. (1990) *Geomorphology in environmental management: a new introduction*, 2nd edition edition. Oxford: Clarendon Press.

Cortes, C. & Vapnik, V. (1995) Support-vector networks. *Machine Learning*, 20, 273–297. https://doi.org/10.1007/BF00994018

Dallaire, C.O., Lehner, B., Sayre, R. & Thieme, M. (2019) A multidisciplinary framework to derive global river reach classifications at high spatial resolution. *Environmental Research Letters*, 14, 024003. https://doi.org/10.1088/1748-9326/aad8e9

Datry, T., Bonada, N. & Boulton, A.J. (2017) What are intermittent rivers and ephemeral streams (IRES)? In: Datry, T., Bonada, N. & Boulton, A. J. (Eds.) *Intermittent Rivers and Ephemeral Streams. Ecology and Management*. Oxford: Elsevier, pp. 01–16.

Datry, T., Boulton, A.J., Bonada, N., Fritz, K., Leigh, C., Sauquet, E. et al. (2018) Flow intermittence and ecosystem services in rivers of the Anthropocene. *Journal of Applied Ecology*, 55, 353–364. https://doi.org/10.1111/1365-2664.12941

Datry, T., Larned, S.T. & Tockner, K. (2014) Intermittent rivers: A challenge for freshwater ecology. *Bioscience*, 64, 229–235. https://doi.org/10.1093/biosci/bit027

Demarchi, L., Bizzi, S. & Piégay, H. (2016) Hierarchical object-based mapping of riverscape units and in-stream mesohabitats using LiDAR and VHR imagery. *Remote Sensing*, 8, 97. https://doi.org/10.3390/rs8020097

Demarchi, L., Bizzi, S. & Piégay, H. (2017) Regional hydromorphological characterization with continuous and automated remote sensing analysis based on VHR imagery and low-resolution LiDAR data. *Earth Surface Processes and Landforms*, 42, 531–551. https://doi.org/10.1002/esp.4092

Demarchi, L., van de Bund, W. & Pistocchi, A. (2020) Object-based ensemble learning for pan-European riverscape units mapping based on Copernicus VHR and EU-DEM data fusion. *Remote Sensing*, 12, 1222. https://doi.org/10.3390/rs12071222

Downs, P.W. & Brookes, A. (1994) Developing a standard geomorphological approach for the appraisal of river projects. In: Kirby, C. & White, W.R. (Eds.) *Integrated River Basin Development*. Chichester: John Wiley & Sons, pp. 299–310.

Downs, P.W. & Gregory, K.J. (2004) *River Channel Management: Towards Sustainable Catchment Hydrosystems*. London: Arnold.

Downs, P.W. & Thorne, C.R. (1996) The utility and justification of river reconnaissance surveys. *Transactions of the Institute of British Geographers, New Series*, 21, 455–468.

England, J. & Gurnell, A.M. (2016) Incorporating catchment to reach scale processes into hydromorphological assessment in the UK. *Water and Environment Journal*, 30, 22–30. https://doi.org/10.1111/wej.12172

European Commission (EC). (2000) *Directive 2000/60/EC of the European Parliament and of the Council of 23 October 2000 establishing a framework for Community action in the field of water policy*. Luxembourg: Office for Official Publications of the European Communities.

European Commission (EC). 2003. Common Implementation Strategy for the Water Framework Directive (2000/60/EC). Guidance Document No. 10: River and lakes – Typology, reference conditions and classification systems. Luxembourg: Office for Official Publications of the European Communities http://ec.europa.eu/environment/water/waterframework/facts_figures/guidance_docs_en.htm (accessed 15 February 2021).

Fryirs, K. (2013) (Dis)Connectivity in catchment sediment cascades: A fresh look at the sediment delivery problem. *Earth Surface Processes and Landforms*, 38, 30–46. https://doi.org/10.1002/esp.3242

Fryirs, K. & Brierley, G.J. (2010) Antecedent controls on river character and behaviour in partly confined valley settings: Upper Hunter catchment, NSW, Australia. *Geomorphology*, 117, 106–120. https://doi.org/10.1016/j.geomorph.2009.11.015

Fryirs, K.A. & Brierley, G.J. (2016) Assessing the geomorphic recovery potential of rivers: forecasting future trajectories of adjustment for use in management. *WIREs Water*, 3, 727–748. https://doi.org/10.1002/wat2.1158

Gallart, F., Cid, N., Latron, J., Llorens, P., Bonada, N., Jeuffroy, J. et al. (2017) TREHS: An open-access software tool for investigating and evaluating temporary river regimes as a first step for their ecological status assessment. *Science of the Total Environment*, 607-608, 519–540. https://doi.org/10.1016/j.scitotenv.2017.06.209

Gallart, F., Prat, N., García-Roger, E.M., Latron, J., Rieradevall, M., Llorens, P. et al. (2012) A novel approach to analysing the regimes of temporary streams in relation to their controls on the composition and structure of aquatic biota. *Hydrology and Earth System Sciences*, 16(9), 3165–3182. https://doi.org/10.5194/hess-16-3165-2012

Gao, B. (1996) NDWI—A normalized difference water index for remote sensing of vegetation liquid water from space. *Remote Sensing of Environment*, 58, 257–266. https://doi.org/10.1016/S0034-4257(96)00067-3

Gilvear, D.J., Davids, C. & Tyler, A.N. (2004) The use of remotely sensed data to detect channel hydromorphology; River Tummel, Scotland. *River Research and Applications*, 20, 795–811. https://doi.org/10.1002/rra.792

Grabowski, R.C. & Gurnell, A.M. (2016) Using historical data in fluvial geomorphology. In: Kondolf, G. & Piégay, H. (Eds.) *Tools in Fluvial Geomorphology*. Hoboken, NJ: John Wiley & Sons, pp. 56–75.

Grant, G.E. & Swanson, F.J. (1995) Morphology and Processes of Valley Floors in Mountain Streams, Western Cascades, Oregon. In: Costa, J. E., Miller, A.J., Potter, K.W. & Wilcock, P.R. (Eds.) *Natural and Anthropogenic Influences in Fluvial Geomorphology*. Washington, DC: American Geophysical Union (AGU), pp. 83–101.

Gregory, K.J. & Park, C. (1974) Adjustment of river channel capacity downstream from a reservoir. *Water Resources Research*, 10, 870–873. https://doi.org/10.1029/WR010i004p00870

Gregory, S.V., Swanson, F.J., McKee, W.A. & Cummins, K.W. (1991) An Ecosystem Perspective of Riparian Zones. *Bioscience*, 41, 540–551. https://doi.org/10.2307/1311607

Guertault, L., Camenen, B., Paquier, A. & Peteuil, C. (2018) A one-dimensional process-based approach to study reservoir sediment dynamics during management operations. *Earth Surface Processes and Landforms*, 43, 373–386. https://doi.org/10.1002/esp.4249

Gurnell, A.M., Rinaldi, M., Belletti, B., Bizzi, S., Blamauer, B. & Braca, G. (2016) A multi-scale hierarchical framework for developing understanding of river behaviour to support river management. *Aquatic Sciences*, 78, 1–16. https://doi.org/10.1007/s00027-015-0424-5

Haralick, R.M., Shanmugam, K. & Dinstein, I. (1973) Textural features for image classification. *IEEE Transactions on Systems, Man, and Cybernetics*, SMC-3, 610–621. https://doi.org/10.1109/TSMC.1973.4309314

Henshaw, A.J., Sekarsari, P.W., Zolezzi, G. & Gurnell, A.M. (2020) Google Earth as a data source for investigating river forms and processes: Discriminating river types using form-based process indicators. *Earth Surface Processes and Landforms*, 45, 331–344. https://doi.org/10.1002/esp.4732

Hooke, J. (1997) Styles of channel change. In: Hey, R.D., Thorne, C.R. & Newson, M.D. (Eds.) *Applied Fluvial Geomorphology for River Engineering and Management*. Chichester: John Wiley & Sons, pp. 237–268.

Hooke, J. (2003) Coarse sediment connectivity in river channel systems: A conceptual framework and methodology. *Geomorphology*, 56, 79–94. https://doi.org/10.1016/S0169-555X(03)00047-3

Hupp, C.R. & Osterkamp, W.R. (1996) Riparian vegetation and fluvial geomorphic processes. *Geomorphology*, 14, 277–295. https://doi.org/10.1016/0169-555X(95)00042-4

Jaeger, K.L., Sutfin, N.A., Tooth, S., Michaelides, K. & Singer, M. (2017) Geomorphology and sediment regimes of intermittent rivers and ephemeral streams. In: Datry, T., Bonada, N. & Boulton, A. (Eds.) *Intermittent Rivers and Ephemeral Streams*. Cambridge, MA: Academic Press, pp. 21–49.

Knighton, A.D. (1999) Downstream variation in stream power. *Geomorphology*, 29, 293–306. https://doi.org/10.1016/S0169-555X(99)00015-X

Kondolf, G.M. (1994) Geomorphic and environmental effects of instream gravel mining. *Landscape and Urban Planning*, 28, 225–243. https://doi.org/10.1016/0169-2046(94)90010-8

Kondolf, G.M. (1995) Geomorphological stream channel classification in aquatic habitat restoration: Uses and limitations. *Aquatic Conservation: Marine and Freshwater Ecosystems*, 5, 127–141. https://doi.org/10.1002/aqc.3270050205

Kuhn, M. (2020) caret: Classification and Regression Training. R package version 6.0-30. In: R Core Team, 2014.

Leigh, C., Boulton, A.J., Courtwright, J.L., Fritz, K., May, C.L., Walker, R.H. & Datry, T. (2016) Ecological research and management of intermittent rivers: An historical review and future directions. *Freshwater Biology*, 61, 1181–1199. https://doi.org/10.1111/fwb.12646

Leinenkugel, P., Deck, R., Huth, J., Ottinger, M. & Mack, B. (2019) The potential of open geodata for automated large-scale land use and land cover classification. *Remote Sensing*, 11, 2249. https://doi.org/10.3390/rs11192249

Leopold, L.B., Wolman, M.G. & Miller, J.P. (1964) *Fluvial Processes in Geomorphology*. San Francisco, CA: W.H. Freeman and Company.

Leviandier, T., Alber, A., Le Ber, F. & Piégay, H. (2012) Comparison of statistical algorithms for detecting homogeneous river reaches along a longitudinal continuum. *Geomorphology*, 138, 130–144. https://doi.org/10.1016/j.geomorph.2011.08.031

Llasat, M.C. & Puigcerver, M. (1990) Cold air pools over Europe. *Meteorology and Atmospheric Physics*, 42, 171–177. https://doi.org/10.1007/BF01314823

Machado, M.J., Medialdea, A., Calle, M., Rico, M.T., Sánchez-Moya, Y., Sopeña, A. & Benito, G. (2017) Historical palaeohydrology and landscape resilience of a Mediterranean rambla (Castellón, NE Spain): Floods and people. *Quaternary Science Reviews*, 171, 182–198. https://doi.org/10.1016/j.quascirev.2017.07.014

Manning, A., Julian, J.P. & Doyle, M.W. (2020) Riparian vegetation as an indicator of stream channel presence and connectivity in arid environments. *Journal of Arid Environments*, 178, 104167. https://doi.org/10.1016/j.jaridenv.2020.104167

Marceau, D.J., Howarth, P.J., Dubois, J.M. & Gratton, D.J. (1990) Evaluation of the grey-level co-occurrence matrix method for land-cover classification using spot imagery. *IEEE Transactions on Geoscience and Remote Sensing*, 28, 513–519. https://doi.org/10.1109/TGRS.1990.572937

Martínez-Fernández, V., González del Tánago, M. & García de Jalón, D. (2019) Selecting geomorphic variables for automatic river segmentation: Trade-offs between information gained and effort required. *Geomorphology*, 329, 248–258. https://doi.org/10.1016/j.geomorph.2019.01.005

Martínez-Fernández, V., Solana-Gutiérrez, J., González del Tánago, M. & García de Jalón, D. (2016) Automatic procedures for river reach delineation: Univariate and multivariate approaches in a fluvial context. *Geomorphology*, 253, 38–47. https://doi.org/10.1016/j.geomorph.2015.09.029

Martín-Vide, J.P., Prats-Puntí, A. & Ferrer-Boix, C. (2020) What controls the coarse sediment yield to a Mediterranean delta? The case of the Llobregat River (NE Iberian Peninsula). *Natural Hazards and Earth System Sciences*, 20, 3315–3331. https://doi.org/10.5194/nhess-20-3315-2020

Mateu, J.F. (1974) La Rambla de la Viuda. Clima e Hidrología. Valencia: Cuadernos de Geografía de la Universitat de València, 47–68.

McManamay, R.A., Troia, M.J., DeRolph, C.R., Sheldon, A.O., Barnett, A.R., Kao, S.-C. & Anderson, M.G. (2018) A stream classification system to explore the physical habitat diversity and anthropogenic impacts in riverscapes of the eastern United States. *PLoS ONE*, 13, e0198439. https://doi.org/10.1371/journal.pone.0198439

Mielke, P.W. (1991) The application of multivariate permutation methods based on distance functions in the earth sciences. *Earth-Science Reviews*, 31, 55–71. https://doi.org/10.1016/0012-8252(91)90042-E

Montgomery, D.R. (1999) Process domains and the river continuum. *Journal of the American Water Resources Association*, 35, 397–410. https://doi.org/10.1111/j.1752-1688.1999.tb03598.x

Montgomery, D.R. & Buffington, J.M. (1997) Channel-reach morphology in mountain drainage basins. *Bulletin of the Geological Society of America*, 109, 596–611. https://doi.org/10.1130/0016-7606(1997)109<0596:CRMIMD>2.3.CO;2

Mueller, E.R. & Pitlick, J. (2005) Morphologically based model of bed load transport capacity in a headwater stream. *Journal of Geophysical Research: Earth Surface*, 110, F02016. https://doi.org/10.1029/2003JF000117

Notebaert, B. & Piégay, H. (2013) Multi-scale factors controlling the pattern of floodplain width at a network scale: The case of the Rhône basin, France. *Geomorphology*, 200, 155–171. https://doi.org/10.1016/j.geomorph.2013.03.014

Papangelakis, E. & Hassan, M.A. (2016) The role of channel morphology on the mobility and dispersion of bed sediment in a small gravel-bed stream. *Earth Surface Processes and Landforms*, 41, 2191–2206. https://doi.org/10.1002/esp.3980

Parker, C., Clifford, N.J. & Thorne, C.R. (2012) Automatic delineation of functional river reach boundaries for river research and applications. *River Research and Applications*, 28, 1708–1725. https://doi.org/10.1002/rra.1568

Phiri, D., Simwanda, M., Salekin, S., Nyirenda, V.R., Murayama, Y. & Ranagalage, M. (2020) Sentinel-2 data for land cover/use mapping: A review. *Remote Sensing*, 12, 2291. https://doi.org/10.3390/rs12142291

Piégay, H., Arnaud, F., Belletti, B., Bertrand, M., Bizzi, S., Carbonneau, P. et al. (2020) Remotely sensed rivers in the Anthropocene: State of the art and prospects. *Earth Surface Processes and Landforms*, 45, 157–188. https://doi.org/10.1002/esp.4787

Pitlick, J., Mueller, E.R., Segura, C., Cress, R. & Torizzo, M. (2008) Relation between flow, surface-layer armoring and sediment transport in gravel-bed rivers. *Earth Surface Processes and Landforms*, 33, 1192–1209. https://doi.org/10.1002/esp.1607

Poff, N.L., Allan, J.D., Bain, M.B., Karr, J.R., Prestegaard, K.L., Richter, B.D. et al. (1997) The Natural Flow Regime. *Bioscience*, 47, 769–784. https://doi.org/10.2307/1313099

R Core Team. (2019) R: A Language and Environment for Statistical Computing. R Foundation for Statistical Computing: Vienna [online]. Available from: https://www.R-project.org/

Rinaldi, M., Surian, N., Comiti, F. & Bussettini, M. (2015) A methodological framework for hydromorphological assessment, analysis and monitoring (IDRAIM) aimed at promoting integrated river management. *Geomorphology*, 251, 122–136. https://doi.org/10.1016/j.geomorph.2015.05.010

Rivas Casado, M., Gonzalez, R.B., Kriechbaumer, T. & Veal, A. (2015) Automated identification of river hydromorphological features using UAV high resolution aerial imagery. *Sensors*, 15, 27969–27989. https://doi.org/10.3390/s151127969

Rivas Casado, M., González, R.B., Ortega, J.F., Leinster, P. & Wright, R. (2017) Towards a transferable UAV-based framework for river hydromorphological characterization. *Sensors*, 17, 2210. https://doi.org/10.3390/s17102210

Rosgen, D.L. (1994) A classification of natural rivers. *Catena*, 22, 169–199. https://doi.org/10.1016/0341-8162(94)90001-9

Rouse, J.W. Jr, Haas, R.H., Schell, J.A. & Deering, D.W. (1974) Monitoring Vegetation Systems in the Great Plains with ERTS. In: Third ERTS Symposium, NASA SP-351, Washington DC, pp. 309–317.

Roux, C., Alber, A., Bertrand, M., Vaudor, L. & Piégay, H. (2015) "FluvialCorridor": A new ArcGIS toolbox package for multiscale riverscape exploration. *Geomorphology*, 242, 29–37. https://doi.org/10.1016/j.geomorph.2014.04.018

Sanchis-Ibor, C., Segura-Beltrán, F. & Almonacid-Caballer, J. (2017) Channel forms recovery in an ephemeral river after gravel mining (Palancia River, Eastern Spain). *Catena*, 158, 357–370. https://doi.org/10.1016/j.catena.2017.07.012

Sanchis-Ibor, C., Segura-Beltrán, F. & Navarro-Gómez, A. (2019) Channel forms and vegetation adjustment to damming in a Mediterranean gravel-bed river (Serpis River, Spain). *River Research and Applications*, 35, 37–47. https://doi.org/10.1002/rra.3381

Schumm, S.A. (1977) *The Fluvial System*. New York: Wiley-Interscience.

Sear, D. & Newson, M.D. (2010) Fluvial geomorphology: its basis and methods. In: Sear, D., Newson, M.D. & Thorne, C.R. (Eds.) *Guidebook of Applied Fluvial Geomorphology*. London: Thomas Telford, pp. 1–31.

Segura, F. & Pardo-Pascual, J.E. (2019) Fan deltas and floodplains in Valencian coastal plains. In: Morales, J. (Ed.) *The Spanish Coastal Systems: Dynamic Processes, Sediments and Management*. Cham: Springer Nature, pp. 489–516.

Segura, F.S. & Camarasa, A. (1996) Balances hídricos de crecidas em ramblas mediterráneas: Pérdidas hídricas. In: Marzol, M.V., Dorta, P. & Valladares, P. (Eds.) *Clima y Agua: la Gestión de un Recurso Climático*. Tenerife: La Laguna University, pp. 235–245.

Simón, J.L., Pérez-Cueva, A.J. & Calvo-Cases, A. (2013) Tectonic beheading of fluvial valleys in the Maestrat grabens (eastern Spain): Insights into slip rates of Pleistocene extensional faults. *Tectonophysics*, 593, 73–84. https://doi.org/10.1016/j.tecto.2013.02.026

Skoulikidis, N.T., Sabater, S., Datry, T., Morais, M.M., Buffagni, A., Dörflinger, G. et al. (2017) Non-perennial Mediterranean rivers in Europe: Status, pressures, and challenges for research and management. *Science of the Total Environment*, 577, 1–18. https://doi.org/10.1016/j.scitotenv.2016.10.147

Spada, D., Molinari, P., Bertoldi, W., Vitti, A. & Zolezzi, G. (2018) Multitemporal image analysis for fluvial morphological characterization with application to Albanian rivers. *ISPRS International Journal of Geo-Information*, 7, 314. https://doi.org/10.3390/ijgi7080314

Sutfin, N.A., Shaw, J.R., Wohl, E.E. & Cooper, D.J. (2014) A geomorphic classification of ephemeral channels in a mountainous, arid region, southwestern Arizona, USA. *Geomorphology*, 221, 164–175. https://doi.org/10.1016/j.geomorph.2014.06.005

Thanh Noi, P. & Kappas, M. (2018) Comparison of Random Forest, k-Nearest Neighbor, and support vector machine classifiers for land cover classification using Sentinel-2 imagery. *Sensors*, 18, 18. https://doi.org/10.3390/s18010018

Thoms, M., Scown, M. & Flotemersch, J. (2018) Characterization of river networks: A GIS approach and its applications. *JAWRA Journal of the American Water Resources Association*, 54, 899–913. https://doi.org/10.1111/1752-1688.12649

Tooth, S. (2000) Process, form and change in dryland rivers: a review of recent research. *Earth-Science Reviews*, 51, 67–107. https://doi.org/10.1016/S0012-8252(00)00014-3

Tucker, C.J. (1979) Red and photographic infrared linear combinations for monitoring vegetation. *Remote Sensing of Environment*, 8, 127–150. https://doi.org/10.1016/0034-4257(79)90013-0

Ward, J.H. (1963) Hierarchical grouping to optimize an objective function. *Journal of the American Statistical Association*, 58, 236–244. https://doi.org/10.1080/01621459.1963.10500845

Whiting, P.J. & Bradley, J.B. (1993) A process-based classification system for headwater streams. *Earth Surface Processes and Landforms*, 18, 603–612. https://doi.org/10.1002/esp.3290180704

Wilcoxon, F. (1945) Individual comparisons by ranking methods. *Biometrics Bulletin*, 1, 80–83.

Williams, G.P. & Wolman, M.G. (1984) *Downstream effects of dams on alluvial rivers*, US Geological Survey, Professional Paper 1286. Washington, DC: US Geological Survey.

Wohl, E. (2017) Connectivity in rivers. *Progress in Physical Geography: Earth and Environment*, 41, 345–362. https://doi.org/10.1177/0309133317714972

Zhang, R. & Zhu, D. (2011) Study of land cover classification based on knowledge rules using high-resolution remote sensing images. *Expert Systems with Applications*, 38, 3647–3652. https://doi.org/10.1016/j.eswa.2010.09.019

Zhang, Z., Murtagh, F., Van Poucke, S., Lin, S. & Lan, P. (2017) Hierarchical cluster analysis in clinical research with heterogeneous study population: Highlighting its visualization with R. *Annals of Translational Medicine*, 5, 75. https://doi.org/10.21037/atm.2017.02.05

SUPPORTING INFORMATION

Additional supporting information may be found in the online version of the article at the publisher's website.

How to cite this article: Rabanaque, M.P., Martínez-Fernández, V., Calle, M. & Benito, G. (2021) Basin-wide hydromorphological analysis of ephemeral streams using machine learning algorithms. *Earth Surface Processes and Landforms*, 1–17. Available from: https://doi.org/10.1002/esp.5250